ADVANCED FUNCTIONAL MATERIALS

www.afm-journal.de

Chemically Functionalized Natural Cellulose Materials for Effective Triboelectric Nanogenerator Development

Chunhua Yao, Xin Yin, Yanhao Yu, Zhiyong Cai, and Xudong Wang**

Cellulose, the most abundant natural polymer, is renewable, biodegradable, and cost competitive. This paper reports the development of a high-performance triboelectric nanogenerator (TENG) with both contacting materials made from cellulosic materials. Cellulose nanofibrils (CNFs) are used as the raw material, and chemical reaction approaches are employed to attach nitro groups and methyl groups to cellulose molecules to change the tribopolarities of CNF, which in turn significantly enhances the triboelectric output. Specifically, the nitro-CNF possesses a negative surface charge density of 85.8 μC m^{-2}, while the methyl-CNF possesses a positive surface charge density of 62.5 μC m^{-2}, reaching 71% and 52% of that for fluorinated ethylene propylene (FEP), respectively. The figure of merit of the nitro-CNF and methyl-CNF is quantified to be 0.504 and 0.267, respectively, comparable to or exceeding a number of common synthetic polymers, such as Kapton, polyvinylidene fluoride, and polyethylene. The TENG fabricated from nitro-CNF paired with methyl-CNF demonstrates an average voltage output of 8 V and current output of 9 μA, which approaches the same level obtained from TENG made from FEP. This work demonstrates a successful strategy of using environmentally friendly, abundant cellulosic materials for replacing the synthetic polymers in TENG development.

1. Introduction

The triboelectric nanogenerator (TENG), an efficient approach to harvest environmental mechanical energy, has been extensively studied since its first demonstration in 2012.[1] It features high power output, flexible structural design, and diverse materials selection.[2,3] Dielectric polymer materials are able to hold surface charges generated from contact electrification and therefore are widely used in TENGs. Typical polymers exploited in TENG are synthetic polymers, such as fluorinated ethylene propylene (FEP),[4,5] poly(methyl methacrylate),[6,7] Kapton,[6,8] and polydimethylsiloxane.[9] Cellulose, on the other hand, is the most abundant natural polymer on Earth. It is widely accessible, biodegradable, and cost competitive.[10,11] If used for TENG development, cellulose nanofibers (CNFs) can lead TENGs to a more green and eco-friendly system that is also naturally degradable, recyclable, and biocompatible. These merits, on the other hand, are nearly unapproachable by the common petroleum-based synthetic polymers that are currently used in TENG designs.

According to the basic working principle of TENG, at least two different materials should be involved that possess different tribopolarity in a triboelectric series after contact electrification.[1,3,12] Typically, the contacting material pairs in TENG are composed of one positive material (e.g., polyamide Al and Cu) and one negative material (e.g., FEP, PTFE (polytetrafluoroethylene), PVDF (polyvinylidene fluoride), and PET (polyethylene terephthalate)).[4,13] Cellulose, of almost neutral relative polarity by its chemical formula, sits at the slightly positive position in the triboelectric series.[1,12] By using CNFs in pair with FEP, we recently demonstrated an effective TENG design that is flexible, transparent, and could be seamlessly integrated with recycled fiber boards.[14] This research opens a new and exciting material engineering direction for TENG development using nature and recyclable materials. However, this work still included synthetic polymer to pair with cellulose for effective charge separation. The weak polarization of nature CNFs results in their limited capability of generating surface charge, which has kept their performance low compared to synthetic polymers. Taking advantage of the abundant hydroxyl groups on cellulose, this work employs chemical reaction approaches to introduce different functionalities, and thus different tribopolarities, to CNFs. The nitro group, an excellent electron-withdrawing functionality, is very likely to acquire negative charge from contact, while the methyl group as an electron-donating functionality is able to be positively charged from contact. Therefore, with pristine CNF as the raw material, we employ chemical reaction approaches to introduce nitro groups and methyl groups to rationally tune the triboelectric polarity of CNF for TENG application. Tribopositive and negative CNF was obtained by the attachment of methyl and nitro groups, respectively. The figure of merit (FOM) of the functionalized CNFs was quantified, which were found comparable to other common synthetic polymers. TENGs fabricated from

C. Yao, X. Yin, Y. Yu, Prof. X. Wang
Department of Materials Science and Engineering
University of Wisconsin-Madison
Madison, WI 53706, USA
E-mail: xudong.wang@wisc.edu
Dr. Z. Cai
Forest Products Laboratory
United State Department of Agriculture Forest Service
Madison, WI 53726, USA
E-mail: zcai@fs.fed.us

DOI: 10.1002/adfm.201700794

the functionalized CNF thin films yielded comparable output with TENGs using FEP, the most triboelectic negative polymers. This work demonstrated the potential of using natural, biodegradable, and low-cost cellulose to create a new type of eco-friendly TENG system.

2. Results and Discussion

Fabrication of CNF film, nitro functionalized-CNF film, and methyl functionalized-CNF film started with synthesizing CNF hydrogel according to our previous method.[14,15] CNF film was obtained by filtering this hydrogel and then drying under pressure. To fabricate nitro-CNF and methyl-CNF films, this CNF hydrogel was freeze dried and then disassembled into fibers for subsequent chemical functionalization. Nitro-CNF fibers were achieved by treating the CNF fibers with a nitration acid mixture made up of HNO_3, H_2SO_4, and water, while methyl-CNF fibers were received by reacting mercerized CNF with dimethyl sulfate. Fourier transform infrared spectroscopy (FTIR) characterization was performed to analyze the chemical structure of the pristine and functionalized CNFs, as shown in **Figure 1**. Their schematic chemical structures are illustrated next to the corresponding FTIR curves. As expected, the pristine CNF (top curve) showed adsorptions of C—O—C stretching within the pyranose ring skeletal (at 1050 cm^{-1}), O—H stretching (3500 cm^{-1}), and C—H stretching (2900 cm^{-1}).[16] For nitro-CNF, the nitration process should render the substitution of hydroxyl groups by nitrate ester groups.[10] Comparing to the pristine CNF, the nitro-CNF (middle curve) presented three new intense peaks positioned at 1638, 1275, and 828 cm^{-1}. They are due to asymmetric and symmetric stretching of the NO_2 group and stretching of the N—O bonds, respectively. Besides, two bands at 747 and 692 cm^{-1} appeared, which can be assigned to the wagging γwNO_2 and the scissoring δNO_2 vibrations, respectively.[17] Furthermore, adsorption intensity of the hydroxyl group in nitro-CNF was significantly reduced in comparison to that of pristine CNF. These observations evidenced that a large number of the hydroxyls on pristine CNF were successfully substituted by the nitro groups. For methyl-CNF, the methylation process should convert the hydroxyls into methoxides.[18] The FTIR spectrum of the as-synthesized methyl-CNF is shown as the bottom curve in Figure 1. The same peaks showed up in methyl-CNF as in pristine CNF; however, the peak intensities were obviously different from before methylation. Since the pyranose ring skeletal in cellulose is untouched during the methylation process, we can compare the intensity of a given peak in different samples by normalizing at 1050 cm^{-1} (C—O—C stretching within the pyranose ring skeletal). It is clear to see that the absorption intensity of O—H stretching in methyl-CNF was notably lower than that in pristine CNF. Meanwhile, the intensity of C—H stretching was higher than that in pristine CNF. This result therefore proved the successful introduction of methyl groups to CNF molecules. The two functionalized CNFs were further processed into thin film morphology. Thickness of the films was controlled to be 100–150 μm by varying the amount of hydrogel/solution. The as-prepared films from pristine and functionalized CNFs were all flexible, transparent, and fairly flat, as shown by the digital photos next to the corresponding molecular models in Figure 1.

X-ray photoelectron spectroscopy (XPS) characterization was implemented on film surfaces to further study the functionalization. Full wavelength survey scan spectra of the pristine, nitro- and methyl-CNF films are shown in **Figure 2**a–c, respectively. All three films presented peaks for O and C, the predominant compositional elements of cellulose. The Na1s peaks came from Na^+, which was introduced during the synthesis of CNF hydrogel by TEMPO ((2,2,6,6 tetramethylpiperidin-1-yl)oxyl) oxidation. In methyl-CNF, the relative peak intensity of C to O was much higher than that in pristine CNF and nitro-CNF, corresponding to the additional of C elements from methylation. The N1s peak appeared in nitro-CNF spectrum, confirming the existence of N element.

The C1s and N1s peaks were further deconvoluted to understand the chemical environment change due to functionalization. The C1s peaks were resolved to four peaks representing

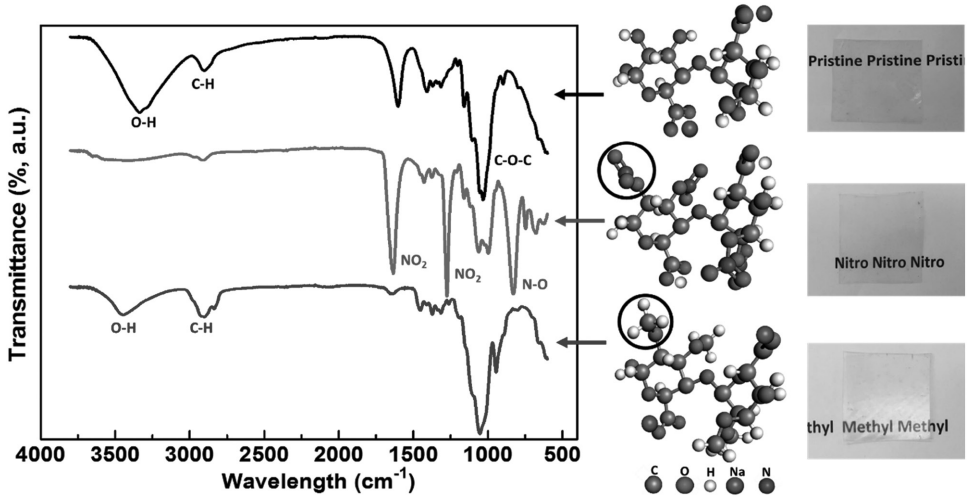

Figure 1. FTIR spectrum and molecular structure of pristine CNF (top row), nitro-CNF (middle row), and methyl-CNF (bottom row). Photos show the transparent films fabricated from these three cellulosic materials.

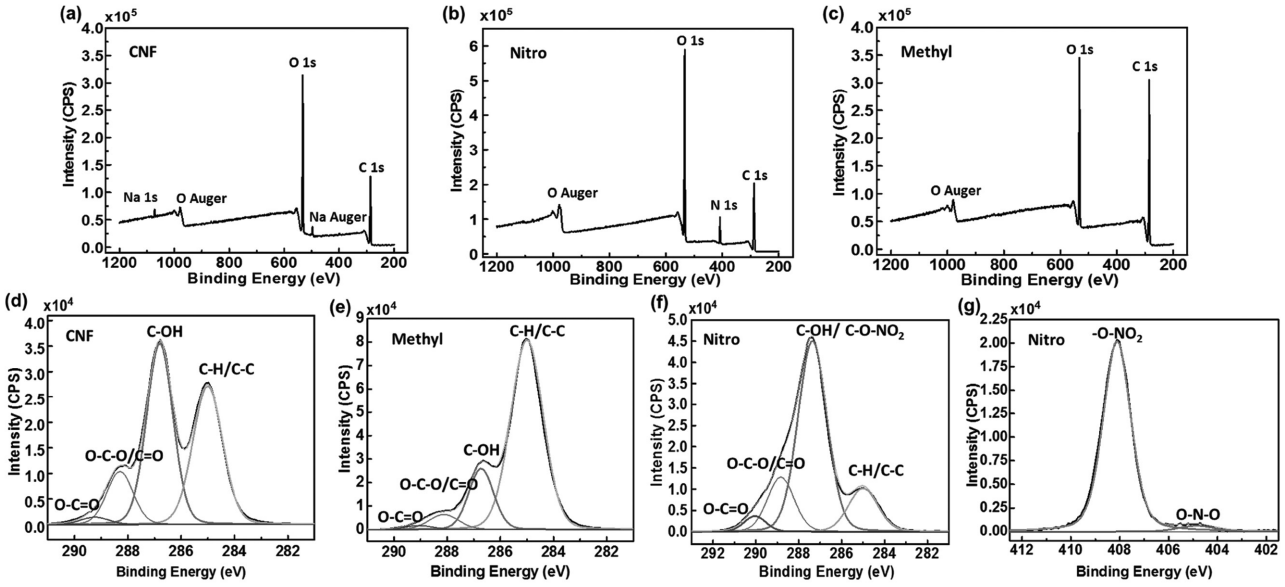

Figure 2. XPS spectrum of pristine CNF, nitro-CNF, and methyl-CNF. a–c) The full spectrum survey of CNF, nitro-CNF, and methyl-CNF, respectively. d–f) High-resolution C1s scan of CNF, methyl-CNF, and nitro-CNF, respectively. g) High-resolution N1s scan of nitro-CNF.

different chemical states of C in cellulose: saturated carbon C1 that has no bonds to oxygen (C—HX, C—C); C2 with one bond to a noncarbonyl oxygen (C—O); C3 with two bonds to oxygen (O—C—O or C=O); and C4 with three bonds (O—C=O) to oxygen. The chemical shifts relative to C1 peak were 1.7 ± 0.2 eV for C2, 3.1 ± 0.3 eV for C3, and 4.4 ± 0.4 eV for C4.[19–21] After deconvolution, the pristine CNF C1s spectrum (Figure 2d) presented two strong peaks at 285 and 286.8 eV and two shoulder peaks at 288.2 and 289.6 eV. They are correspondingly assigned to C—C/C—H bond, C—OH bond, O—C—O bond, and O=C—O bond. This bonding agrees well with literature.[20,22] For methyl-CNF, relative peak intensities of the four deconvoluted peaks were very different from those in pristine CNF (Figure 2e). When the intensity of C3 and C4 peak remained much the same before and after the methylation, the intensity of C1 peak was significantly increased and the C2 peak slightly reduced. This represents the substitution of —OH (C2 peak) with —CH (C1 peak). Combining the XPS and FTIR results, we can conclude that methyl groups were successfully attached on cellulose in the methyl-CNF samples. For nitro-CNF, the C1s peak was deconvoluted to the same four peaks (Figure 2f), where the peak at 286.8 eV should include the contributions from the carbon connected to nitrate ester group since this carbon is singly bonded to a noncabonyl oxygen.[21,23] By comparing pristine CNF and nitro-CNF, it could be clearly seen that the relative intensity of C2, C3, and C4 peaks remained much the same before and after the nitro functionalization. This is self-explanatory since the nitrate ester groups only substitute the hydroxyls in cellulose, and carbon connected to both nitrate ester groups and hydroxyl groups contributed to the same C2 peak. Further, the N1s spectrum of nitro-CNF was deconvoluted to a predominant peak at 408.1 eV and a wide band centered at 404.8 eV (Figure 2g). They were originated from the nitrate ester groups (—O—NO_2) and nitrite ester groups (—O—NO), respectively, and the latter is a byproduct in the nitration process.[23] Through the above analysis, we can conclude that nitro groups were successfully attached to the cellulose molecules in the nitro-CNF samples. Films fabricated from the functionalized CNFs presented a uniform element distribution across the entire thickness, as shown by the Energy Dispersive Spectroscopy (EDS) mapping of the film cross-section (Figure S1, Supporting Information). This phenomenon is a result of complete CNF functionalization, which is favorable for maximizing the property tuning of the entire CNF films.

Triboelectric surface charge density σ is a critical factor that determines the output performance of TENG devices. It was formulated that σ is the only material-related parameter in the expression for TENG performance FOM,[24] and the optimization of σ would significantly enhance the TENG performance since the FOM is given by the squared value of normalized triboelectric surface charge density. Therefore, σ was characterized from the three types of CNF-based films to evaluate their potential as TENG-active materials. A homemade setup (inset of **Figure 3**a) was employed for the measurements, where Ga-In eutectic liquid metal was used as one triboelectrification material. The charge transfer between CNF film and the liquid metal electrode was measured by contacting and separating the film and metal electrodes in a controlled manner (see the Experimental Section for details). Corresponding current peaks obtained from the CNF, FEP, nitro-CNF, and methyl-CNF films during a contact-separation cycle with Ga-In are shown in Figure 3a–d, respectively. The current peaks were measured to be -15.9×10^{-3}, 144.5×10^{-3}, 102.6×10^{-3}, and -74.7×10^{-3} μA, and the corresponding charge density was calculated to be −13.3, 120.9, 85.8, and −62.5 μC m^{-2}, respectively (**Table 1**). The FEP film was used here as a benchmark to evaluate the property of the CNF-based films. The obtained charge density value of FEP is very close to the reported value (133.24 μC m^{-2} for FEP against Galinstan) in ref. [24], confirming the validity of our measurement. The negative sign for CNF and methyl-CNF

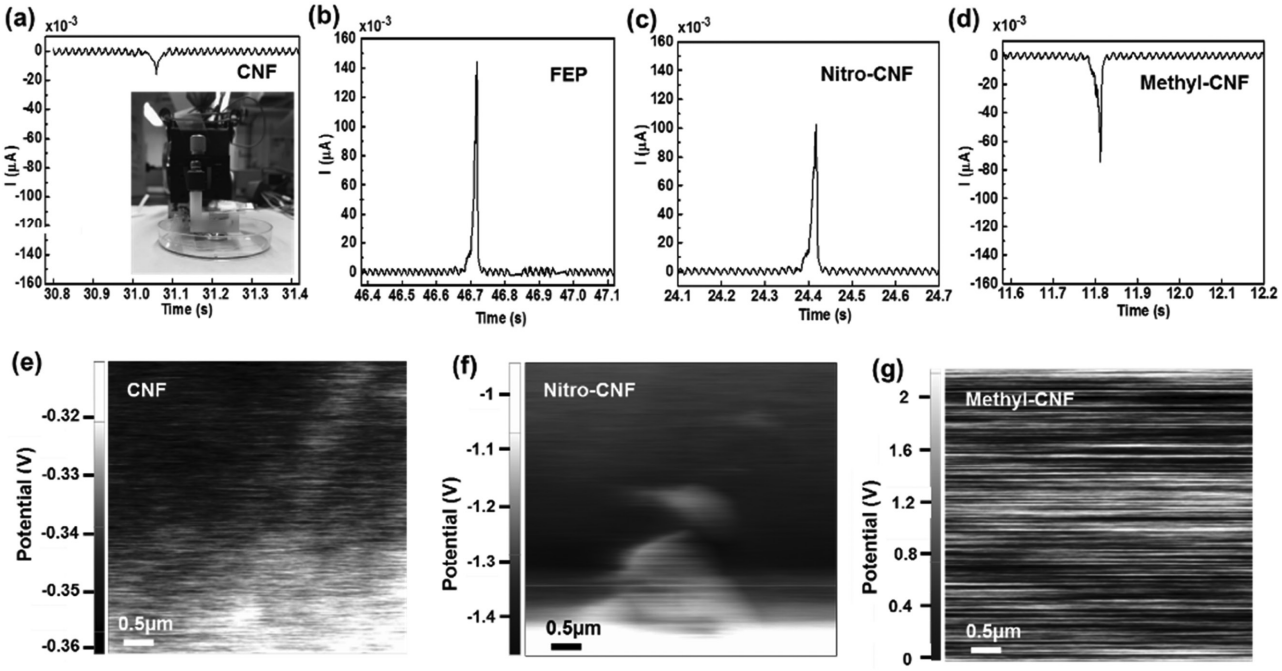

Figure 3. Current flow measured during one contact-separation event when electric contact was made between Ga-In eutectic liquid metal and the triboelectric film of a) CNF, b) FEP, c) nitro-CNF, and d) methyl-CNF. Inset in (a) is the setup that can move vertically for making the contacts. The SKPM surface potential mapping of e) pristine CNF, f) nitro-CNF, and g) methyl-CNF.

suggests that electrons were transferred from CNF/methyl-CNF to Ga-In during the contact, i.e., the triboelectric surface potential of CNF and methyl-CNF was positive. On the other hand, the triboelectric surface potential of FEP and nitro-CNF was negative. These results are in accordance with the materials nature. CNF is slightly tribopositive due to the intrinsic abundant oxygen atoms in cellulose and the small amount of carboxylic groups produced from the nanofibrillation processing of cellulose pulp. Methyl-CNF is also tribopositive because of the electron-donating methyl groups. Nitro-CNF is tribonegative since it carries strong electron-withdrawing nitro groups.

Comparing the value before and after the chemical functionalization, one can clearly see that nitration and methylation significantly increased the triboelectric surface potential of CNF films by a factor of ≈4–6. Besides, both positive and negative tribopolarities were obtained after functionalizing the slightly positive CNF, suggesting that one can rationally engineer the polarity of CNF-based films by controlling the attached functional groups. By normalizing the charge density values of the CNF-based films to that of FEP, the relative triboelectric charge densities (σN) of CNF, nitro-CNF, and methyl-CNF were found to be −0.110, 0.710, and −0.517, respectively. The square of σN gave the FOMs of nitro-NC (0.504) and methyl-NC (0.267), which are comparable and even superior to other commonly used synthetic triboelectric polymers such as Kapton (0.36), PVDF (0.20), and polyethylene (0.18).[24]

The surface potential of CNF-based films was further mapped by noncontact scanning Kelvin probe microscopy (SKPM). The SKPM mapping revealed that the pristine CNF has an average surface potential of ≅330 mV (Figure 3e). As a result of its strong triboelectric negative polarity, nitro-CNF showed a significantly more negative surface potential of ≅1.3 V (Figure 3f), which approached much closer to the value of FEP surface (≅2.2 V, Figure S3, Supporting Information). The high triboelectric positive polarity of the methyl-CNF brought its surface potential to a very positive value of ≈1.1 V (Figure 3g). The large variation of the surface potential values further evidenced the effective and remarkable electronic property tuning by the nitration and methylation processing of natural CNF.

To evaluate the performance enhancement enabled by the CNF functionalization, the three CNF-based films and the FEP film were separately assembled against Cu electrode into

Table 1. Triboelectric properties of pristine and functionalized CNF films in comparison to an FEP film and corresponding TENG output performance when paired with Cu.

Material	Surface charge density [μC m^{-2}]	Normalized triboelectric charge density (σN)	Figure of merit (FOM)	Average voltage output from TENG when paired with Cu [V]	Average current output from TENG when paired with Cu [μA]
FEP	120.9	1	1	6.9	7.8
CNF	−13.3	−0.11	0.012	0.9	0.8
Nitro-CNF	85.8	0.71	0.504	4.9	5.0
Methyl-CNF	−62.5	−0.52	0.267	3.7	3.9

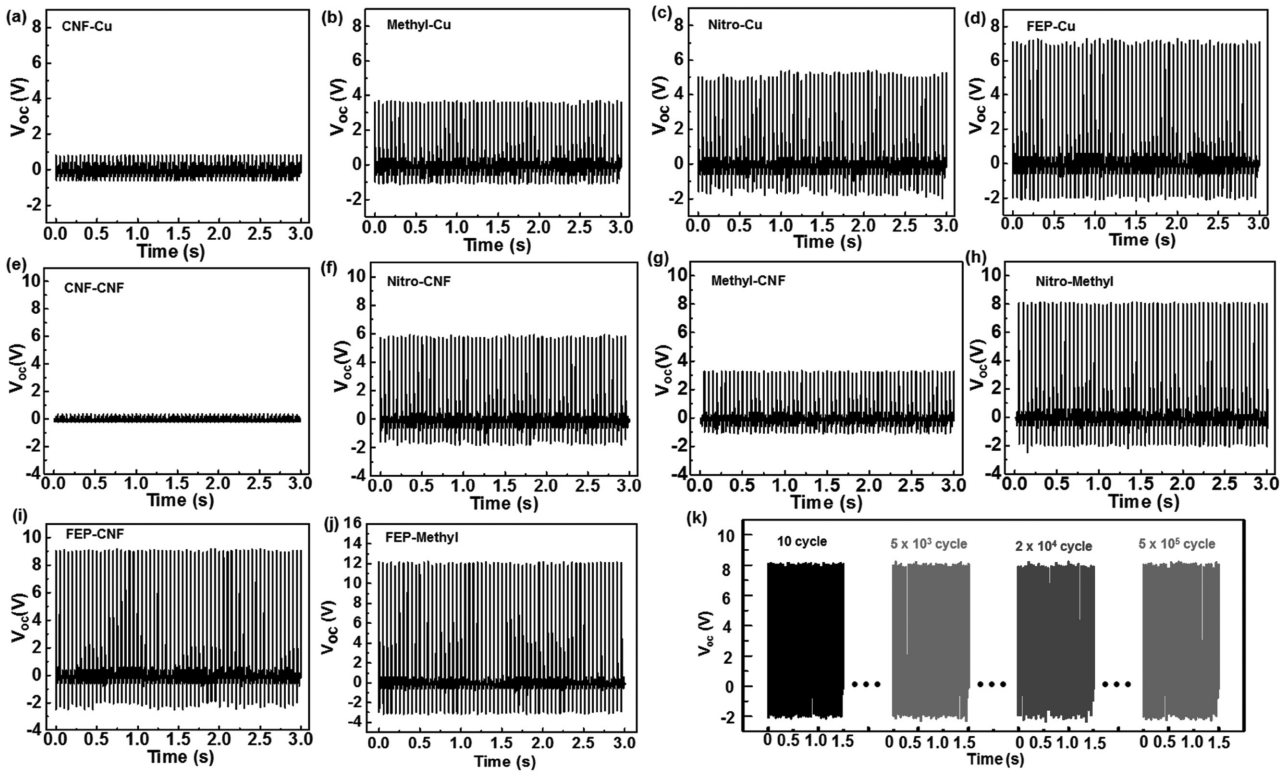

Figure 4. Voltage output of TENGs made from various film pairs of a) CNF/Cu, b) methyl-CNF/Cu, c) nitro-CNF/Cu, d) FEP/Cu, e) CNF/CNF, f) nitro-CNF/CNF, g) methyl-CNF/CNF, h) nitro-CNF/methyl-CNF, i) FEP/CNF, and j) FEP/methyl-CNF. k) The long-term voltage output of the TENG made from nitro-CNF/methyl-CNF pair.

TENG devices. Triboelectric output was measured based on a simple vertical contacting design. Voltage outputs of these four devices are shown in **Figure 4**a–d and corresponding current outputs are included in Figure S2 (Supporting Information). The average voltage outputs and current outputs were summarized in Table 1. Because Cu is slightly triboelectric negative, the pristine CNF-Cu pair showed a very small average voltage of ≈0.8 V and current of ≈0.8 μA. The electric outputs obtained from nitro-CNF-Cu and methyl-CNF-Cu pairs were significantly higher, with an average voltage and current of 4.9 V/5.0 μA and 3.7 V/3.9 μA, respectively. These values are close to the highest output obtained from the FEP-Cu pair (≈6.9 V in voltage and ≈7.8 μA in current), which clearly proved that the chemical functionalization could appreciably promote the triboelectric performance of nature CNF films.

The remarkable triboelectric polarity tuning allowed the creation of all-CNF-based TENGs with both triboelectric functional layers being CNF materials. TENGs with the vertical contact mode were assembled with different pairs of pristine and functionalized CNF, and their voltage and current outputs were measured under the same mechanical impact conditions as the CNF-Cu systems. As expected, the output from a pair of pristine CNF films was nearly negligible (Figure 4e and Figure S2e, Supporting Information). The two chemically functionalized CNF films both showed enhanced output when paired with the pristine CNF film. Nitro-CNF exhibited a high output of 5.9 V and 6.8 μA (Figure 4f and Figure S2f, Supporting Information). The output from methyl-CNF was about half of that from nitro-CNF (3.3 V and 4.3 μA, as shown in Figure 4g and Figure S2g, Supporting Information). Because nitro- and methyl-functionalization shifted the triboelectric polarization toward opposite directions, when these two materials were paired together, the output was further to an average voltage and current value of 8 V and 9 μA, respectively (Figure 4h and Figure S2h, Supporting Information). It is important to notice that output from the nitro-CNF-methyl-CNF pair was approaching that of the FEP-CNF pair (9 V and 10.5 μA, Figure 4i and Figure S2i, Supporting Information), whereas the FEP-methyl-CNF pair showed an even higher output (12 V and 10.5 μA, Figure 4j and Figure S4j, Supporting Information) due to the more positive methyl functionalization. Since this polarization tuning was based on molecular-level functionalization, the enhanced output was fairly stable. A long-term test of the nitro-CNF-methyl-CNF TENG revealed no output signal decay after 5×10^5 cycles (Figure 4k). These experiments evidenced the great potential for replacing commercial synthetic polymers by renewable and biodegradable CNF-based films with comparable triboelectric performance.

3. Conclusion

In conclusion, biodegradable and abundant cellulose nanofibril (CNF) was implemented in TENG development. Nitro groups and methyl groups were successfully introduced on CNF by chemical reaction methods, and these two functionalities

rendered opposite, high tribopolarity of the material. Nitro-CNF and methyl-CNF exhibited a surface charge density of –85.8 and 62.5 μC m^{-2}, respectively, which is significantly larger than –13.3 μC m^{-2} from pristine CNF. These charge density values were corresponding to 71% and 52% of that for FEP, the most triboelectric negative material, while pristine CNF could only reach 11% of FEP. The FOM of the nitro-CNF and methyl-CNF was quantified to be 0.51 and 0.28, respectively. TENGs were assembled by pairing the functionalized CNF tin film with Cu electrode and among each other. Triboelectric output measurements revealed that nitro-CNF and methyl-CNF substantially outperformed pristine CNF in TENG application. When nitro-CNF was paired with methyl-CNF in a TENG device, the output was further raised to a very close value of that produced by the FEP-pristine CNF pair. This work presented a simple, versatile, and scalable chemical functionalization method to obtain high tribopolarity CNF materials. In addition to the functional groups shown in this work, many more groups, such as fluoro group and amino group could also be introduced to CNF molecules, which may render triboelectric polarity to a greater extent. This technique establishes a new processing methodology platform for developing high-performance TENG devices from renewable and cost-effective natural resources.

4. Experimental Section

Fabrication of CNF, Nitro-CNF, and Methyl-CNF Film: CNF hydrogel was synthesized from wood pulp by tetramethylpiperidine-1-oxy (TEMPO)-mediated oxidation and subsequent mechanical homogenization following the procedure in previous publications.[14,15] The final product is a stable 1 wt% hydrogel of CNFs in water. To obtain a CNFs film, an air filtration system (Millipore Corporation, USA) was utilized. In the filtration chamber, CNF hydrogel was filtered through a polytetrafluoroethylene membrane (0.1 μm pore sizes) under 0.55 MPa air pressure. The received CNF filter slab was afterward sandwiched between layers of waxy coated paper, filter paper, and caul plates for room temperature drying followed by 65 °C oven drying to get the final CNF film. Weights were applied on top of the sandwich during drying to prevent warping and wrinkling.

To synthesize nitro functionalized CNF, a nitration acid mixture was prepared by mixing 25 wt% HNO_3, 59.5 wt% H_2SO_4, and 15.5 wt% H_2O at room temperature. Dry CNF fibers obtained from freeze drying the CNF hydrogel were then immersed in the acid at room temperature for 2 h under stirring. 50 mL of acid was used for each gram of CNF. After the reaction, the fibers were retrieved by washing the reactants with deionized (DI) water and centrifugation for several cycles. Then the CNF fibers were distributed in DI water and boiled twice for 1.5 h each time. Subsequently, the CNF fibers were washed twice using DI water containing 0.027% of sodium carbonate. After centrifugation and drying at 60 °C, the obtained fibers were distributed in ethyl acetate, and then the nitro-CNF film was received after the volatilization of ethyl acetate in atmosphere at room temperature.

To fabricate methyl-CNF, 1 g of CNF dry fibers were mercerized in 20 mL 50% NaOH solution for 1 h at room temperature. Then, the fibers were collected by centrifugation to remove the NaOH solution and washed with DI water several times. The fibers were then added into 12 mL dimethyl sulfate solution (3 mL dimethyl sulfate in 9 mL acetone). After reaction for 2 h at room temperature, the system was washed with acetone and centrifuged repeatedly. The collected fibers were dried at 60 °C. The obtained methyl-CNF fibers were then added to DI water by a weight ratio of 2%. The mixture was therefore heated at 90 °C with stirring till the formation of uniform hydrogel. After cooling down to room temperature, this hydrogel was filtered through the same millipore filtration system as used in fabricating CNF films. Final methyl-CNF film was received after drying the wet film at 65 °C overnight.

Assembly of CNF-Based TENGs: All TENGs used in this work were vertical contact type. For TENGs with two active cellulose materials, the active materials with a size of 1 cm × 1 cm were separately attached to the center of two indium tin oxide (ITO) coated PET substrates (2 cm × 5 cm) and aligned face-to-face. The two ITO/PET substrates were separated 2 mm apart by a spacer and connected to the external circuit. TENGs with only one active cellulose material had the bare ITO/PET substrate as the counter electrode. Films studied in this work include CNF, nitro-CNF, methyl-CNF, commercially obtained FEP. Thickness of the CNF films used in TENG characterization was ≈100 μm.

Characterizations: FTIR spectra were measured by a Thermo Nicolet iZ10 with a resolution of 4 cm^{-1}. XPS scan was performed using a Thermos Scientific K-alpha XPS. The spectra were charge corrected by setting the saturated hydrocarbon contribution in C1s emission to 285 eV. Deconvolution of high-resolution spectra was performed on the Thermo Advantage program equipped with the instrument. The fitting was based on 90% Gaussian and 10% Lorentzian curve shapes. Morphology and element analyses were performed on a scanning electron microscope (LEO 1530 Gemini, Zeiss) coupled with energy dispersive spectroscopy system. Surface potential mapping was implemented by noncontact SKPM on XE-70 Park system atomic-force microscopy, using a Cr-Au alloy probe under DC offset potential. Prior to scanning, all film surfaces were cleaned with ethanol followed by air drying to remove contamination.

FOM Determination: FOM was quantified by measuring the relative surface charge density and calculating the squared value of normalized triboelectric charge density (σN) following ref. [24]. Gallium-indium eutectic liquid metal was placed on top of a Cu electrode in a petri dish. The CNF film with an area of 1 cm × 0.75 cm was back pasted with another Cu electrode. These two Cu electrodes were separately connected to the two leads of a Bio-Logic VSP potentiostat. The films were attached on the bottom of an acrylic block that can move freely in vertical direction via a cantilever. The petri dish was fixed on a stable surface and placed right below the testing film. For each contact event, the film was first brought down to make intimate contact with the liquid metal. Then, the two electrodes were short circuited to deplete the potential difference. Thereafter, the film was lifted up from the liquid metal, and the current flow was recorded by the potentiostat during the separation. The corresponding charge transferred was then determined by integrating the current versus time curve.

TENG Characterization: Performance of the cellulose-based TENGs was characterized based on the vertical contacting design by applying periodical vertical force. The top electrode was pressed down by a shaker with 17.8 N force at 20 Hz frequency, and the bottom electrode was fixed on a lab bench. The voltage output was measured using an Agilent DSO1012A oscilloscope with an internal resistance of 1 MΩ, and the current output was recorded by an Autolab PGSTAT302N station.

Supporting Information

Supporting Information is available from the Wiley Online Library or from the author.

Acknowledgements

This work was supported by Wisconsin Alumni Research Foundation (WARF) and USDA Forest Product Laboratory (14-JV-11111124-029).

Conflict of Interest

The authors declare no conflict of interest.

Keywords

cellulose nanofibrils (CNFs), chemical functionalization, methylation, nitration

Received: February 12, 2017
Revised: April 30, 2017
Published online:

[1] F.-R. Fan, Z.-Q. Tian, Z. L. Wang, *Nano Energy* **2012**, *1*, 328.
[2] Z. L. Wang, *ACS Nano* **2013**, *7*, 9533.
[3] Z. L. Wang, J. Chen, L. Lin, *Energy Environ Sci.* **2015**, *8*, 2250.
[4] Y. Zi, J. Wang, S. Wang, S. Li, Z. Wen, H. Guo, Z. L. Wang, *Nat. Commun.* **2016**, *7*, 10987.
[5] S. Wang, Y. Xie, S. Niu, L. Lin, C. Liu, Y. S. Zhou, Z. L. Wang, *Adv. Mater.* **2014**, *26*, 6720.
[6] G. Zhu, C. Pan, W. Guo, C.-Y. Chen, Y. Zhou, R. Yu, Z. L. Wang, *Nano Lett.* **2012**, *12*, 4960.
[7] M. P. Mahmud, J. Lee, G. Kim, H. Lim, K.-B. Choi, *Microelectron. Eng.* **2016**, *159*, 102.
[8] D. Kim, S.-B. Jeon, J. Y. Kim, M.-L. Seol, S. O. Kim, Y.-K. Choi, *Nano Energy* **2015**, *12*, 331.
[9] a) Y. Mao, D. Geng, E. Liang, X. Wang, *Nano Energy* **2015**, *15*, 227; b) Y. Yu, Z. Li, Y. Wang, S. Gong, X. Wang, *Adv. Mater.* **2015**, *27*, 4938; c) Z. H. Lin, G. Cheng, Y. Yang, Y. S. Zhou, S. Lee, Z. L. Wang, *Adv. Funct. Mater.* **2014**, *24*, 2810.
[10] U. Heinze, W. Wagenknecht, *Comprehensive Cellulose Chemistry: Functionalization of Cellulose*, Wiley-VCH, Weinheim **1998**.
[11] S. Ummartyotin, H. Manuspiya, *Renewable Sustainable Energy Rev.* **2015**, *41*, 402.
[12] A. Diaz, R. Felix-Navarro, *J. Electrostat.* **2004**, *62*, 277.
[13] a) Y. Zhu, B. Yang, J. Liu, X. Wang, L. Wang, X. Chen, C. Yang, *Sci. Rep.* **2016**, *6*, 22233; b) L. Dhakar, S. Gudla, X. Shan, Z. Wang, F. E. H. Tay, C.-H. Heng, C. Lee, *Sci. Rep.* **2016**, *6*, 22253; c) T. Huang, M. Lu, H. Yu, Q. Zhang, H. Wang, M. Zhu, *Sci. Rep.* **2015**, *5*, 13942; d) Y. Yang, H. Zhang, R. Liu, X. Wen, T. C. Hou, Z. L. Wang, *Adv. Energy Mater.* **2013**, *3*, 1563; e) G. Zhu, Y. S. Zhou, P. Bai, X. S. Meng, Q. Jing, J. Chen, Z. L. Wang, *Adv. Mater.* **2014**, *26*, 3788; f) Y. Yang, G. Zhu, H. Zhang, J. Chen, X. Zhong, Z.-H. Lin, Y. Su, P. Bai, X. Wen, Z. L. Wang, *ACS Nano* **2013**, *7*, 9461; g) F.-R. Fan, L. Lin, G. Zhu, W. Wu, R. Zhang, Z. L. Wang, *Nano Lett.* **2012**, *12*, 3109; h) B. Meng, W. Tang, Z. Too, X. Zhang, M. Han, W. Liu, H. Zhang, *Energy Environ. Sci.* **2013**, *6*, 3235; i) L. Zhang, F. Xue, W. Du, C. Han, C. Zhang, Z. Wang, *Nano Res.* **2014**, *7*, 1215.
[14] C. Yao, A. Hernandez, Y. Yu, Z. Cai, X. Wang, *Nano Energy* **2016**, *30*, 103.
[15] C. Yao, F. Wang, Z. Cai, X. Wang, *RSC Adv.* **2016**, *6*, 92648.
[16] a) T. Kondo, C. Sawatari, *Polymer* **1996**, *37*, 393; b) H. Yang, R. Yan, H. Chen, D. H. Lee, C. Zheng, *Fuel* **2007**, *86*, 1781.
[17] V. Kovalenko, R. Mukhamadeeva, L. Maklakova, N. Gustova, *J. Struct. Chem.* **1994**, *34*, 540.
[18] a) R. L. Oliveira, J. G. Vieira, H. S. Barud, R. Assunção, G. R Filho, S. J. Ribeiro, Y. Messadeqq, *J. Braz. Chem. Soc.* **2015**, *26*, 1861; b) P. L. Nasatto, F. Pignon, J. L. Silveira, M. E. R. Duarte, M. D. Noseda, M. Rinaudo, *Polymers* **2015**, *7*, 777; c) R. G. Viera, G. R. Filho, R. M. de Assunção, C. da Silva Meireles, J. G. Vieira, G. S. de Oliveira, *Carbohydr. Polym.* **2007**, *67*, 182.
[19] a) L. S. Johansson, J. Campbell, *Surf. Interface Anal.* **2004**, *36*, 1018; b) A. Dufresne, *Nanocellulose: From Nature to High Performance Tailored Materials*, Walter de Gruyter, Berlin, **2013**; c) M. Božič, P. Liu, A. P. Mathew, V. Kokol, *Cellulose* **2014**, *21*, 2713; d) C. Viornery, Y. Chevolot, D. Léonard, B.-O. Aronsson, P. Péchy, H. J. Mathieu, P. Descouts, M. Grätzel, *Langmuir* **2002**, *18*, 2582.
[20] M. Ghanadpour, F. Carosio, P. T. Larsson, L. Wagberg, *Biomacromolecules* **2015**, *16*, 3399.
[21] B. C. Beard, *Appl. Surf. Sci.* **1990**, *45*, 221.
[22] M. Gopiraman, H. Bang, G. Yuan, C. Yin, K.-H. Song, J. S. Lee, I. M. Chung, R. Karvembu, I. S. Kim, *Carbohydr. Polym.* **2015**, *132*, 554.
[23] D. Clark, P. Stephenson, *Polymer* **1982**, *23*, 1034.
[24] Y. Zi, S. Niu, J. Wang, Z. Wen, W. Tang, Z. L. Wang, *Nat. Commun.* **2015**, *6*, 8376.

